CHAPTER 9

CHARACTERIZATION OF Sb_2Te_3 AND Sb_2Te_3 BASED ALLOY CRYSTALS

The main facets of characterization of crystals are;

(a) the chemical composition

(b) the geometrical or structural arrangement of atoms in the crystal and

(c) the electronic state of the crystal.

The experimental tools which are useful for the basic characterization of a crystal are discussed in Chapter 3. Several techniques have been employed by different authors to characterize the thermoelectric materials. Ivanova et al.[1] studied the cleavage surfaces of single crystals of Sb_2Te_3 and their solid solutions obtained by Czochralski method using electron channeling patterns (ECPs) with scanning electron microscopy. They found the crystallographic direction of growth and the degree of perfection of the seed crystals and single crystals as well as the depth of the layer damaged during cutting from the change in the ECP contrast. Mavlonov et al.[2] have conducted an x-ray spectral microanalysis (EPMA) of antimony telluride single crystals doped with tin and thallium in a scanning mode. They have shown that Sb_2Te_3 single crystals doped with 0.01 mass % Tl and 0.1 – 1 mass % Sn have a uniform impurity distribution. Ivanova et al.[3] used plasma atomic-absorption analysis (Perkin-Elmer analyzer) to determine the compositions of the melt and single crystals of Sb_2Te_3-Bi_2Te_3-Bi_2Se_3.

The present study is limited to evaluation of elemental composition and homogeneity using EDAX and SIMS techniques and to confirm the structure using powder X-ray Diffraction of Sb_2Te_3 and Sb_2Te_3 based alloys.

ENERGY DISPERSIVE ANALYSIS OF X-RAYS (EDAX) STUDY

In the case of III – V's and compounds containing group VI elements, the differences in vapour pressure and reactivity of the volatile components result in

change of the stoichiometry of the melt. This change in turn corresponds to the changes in other properties of the material (crystal). The present day understanding of the properties of the thermoelectric material is dependent on complete chemical analysis which encompasses various aspects including identification of various elements present, quantitative chemical composition, chemical state of the elements and distribution of each element over the surface. While stoichiometry control, or the ability to maintain precisely controlled vapour pressure in order to effect melt and hence crystal stoichiometry, is a desirable feature of any technique, contamination is a basic limitation in all melt growth methods, the most troublesome limitation being that caused by the reactivity of the silica. However, it is not the purpose here to discuss the techniques concerned with stoichiometric or near stoichiometric melt growth. The present study concentrates on the detection and quantitative and distributional analysis of the components present in the Bridgman grown crystals, viz., $Bi_xSb_{2-x}Te_3$ (x = 0, 0.2, 0.5, 1) and $In_{0.2}Sb_{1.8}Te_3$. Further the extent of contamination caused by the reactivity of the crucible (silica) is also quantitatively evaluated. The compositional analysis has been done by the Energy Dispersive Analysis of X-rays (EDAX). It is an attachment to the advanced electron microscope for chemical analysis. The principle underlying EDAX is as follows: When the beam of electrons strikes a specimen, a fraction of the incident electrons excites the atoms of the specimen which then emits X-rays strictly related to the atomic number of the elements excited and thereafter their deflection forms the basis of elemental analysis. EDAX gives information about chemical composition or phases in which they exist.

Horak et al.[4] have used EDAX to determine the non-stoichiometry of Sb_2Te_3 crystals and found that the average composition corresponds to the formula $Sb_2Te_{2.948}$. Mzerd et al.[5] have shown that Sb_2Te_3 is usually non-stoichiometric and annealing in N_2 and H_2 results in improved stoichiometry which is explained by the out-diffusion of excess Sb.

In the present study, LINK ISIS-2000 EDX analyser equipped with scanning microscope [JEOL 840] has been used to make quantitative analysis of the composition and to check the stoichiometry of the system. It is an advanced electron microscope with resolution of 4 nm and magnification of 10X to 300,000X. The equipment provides qualitative and quantitative information on all elements with atomic number (Z) greater than 12 (Mg).

Fig. 1 shows the Energy Dispersive Spectra (EDS) of $BiSbTe_3$ single crystal. Table 1 shows the atomic % of Sb, Bi, In and Te in $Bi_xSb_{2-x}Te_3$ (x = 0, 0.2, 0.5, 1) and $In_{0.2}Sb_{1.8}Te_3$ crystals as obtained with these spectra. It is observed that the composition of the crystal under study deviates from the stoichiometry. Tellurium on an average has been observed to exist 2.5% more than that expected in the case of alloys of Sb_2Te_3. It is known that for the crystals grown by the Bridgman technique, the presence of Si is due to the diffusion from Silica ampoule into the crystal. Hence, the atomic % of Si and its distribution into different regions of the sample were also obtained. Table 2 shows the atomic % of the elements in $BiSbTe_3$ at three different regions of the same sample for a spot size of 7.5 nm under a magnification of 3000X . Also, the distribution of Silicon along the surface is given in Table 2. On an average, Si is present to an extent of about 1.7 atomic % and Te is observed to be less by about the same % age. In the alloyed compounds, apparently the Te content is in an excess as observed in Table 1. However, when subjected to Si analysis this excess actually corresponds to Si as exemplified by an analysis of $BiSbTe_3$ given in Table 2. Thus it is seen that the stoichiometric deviation in the Te content is not unusual as reported by Horak et al.[4].

X-RAY DIFFRACTION STUDY

Of at least equal importance to the chemical nature – the identity and quantity of the atoms present in a crystal – is the physical perfection – the position of the atoms in a crystal. The cornerstone and beginning of such work is the accurate determination of structure with x-ray diffraction.

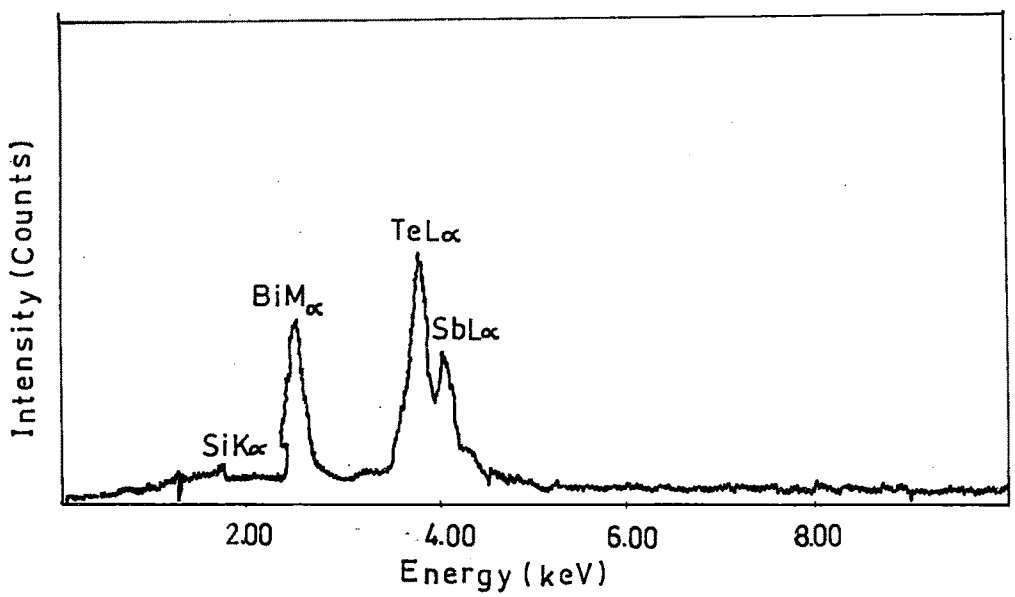

Fig.1. Energy Dispersive Spectra of $BiSbTe_3$ Single Crystal.

TABLE 1

Compositional Analysis of Sb_2Te_3 and Sb_2Te_3 based crystals

Crystal	Elements present	Atomic %
Sb_2Te_3	Sb	40.23
	Te	59.77
$Bi_{0.2}Sb_{1.8}Te_3$	Bi	3.2
	Sb	35.06
	Te	61.74
$Bi_{0.5}Sb_{1.5}Te_3$	Bi	10.10
	Sb	28.62
	Te	61.29
$BiSbTe_3$	Bi	19.05
	Sb	19.61
	Te	61.34
$In_{0.2}Sb_{1.8}Te_3$	In	4.03
	Sb	33.93
	Te	62.04

TABLE 2

Compositional Analysis of 3 Different Regions from $BiSbTe_3$ Crystal

$BiSbTe_3$	Elements present	Atomic %
Region 1	Si	2.216
	Bi	19.609
	Sb	18.289
	Te	59.886
Region 2	Si	1.476
	Bi	20.231
	Sb	19.028
	Te	59.265
Region 3	Si	1.522
	Bi	24.009
	Sb	15.845
	Te	58.625

X-ray diffraction techniques are useful tools for structural investigations of bulk and thin films. The powder x-ray diffraction technique in particular, has been used for structural analysis.

Amin et al.[6] have used metallographic techniques in conjunction with X-ray powder diffraction pattern to assess the homogeneity of the pseudo-binary and ternary alloys (75% Sb_2Te_3-25%Bi_2Te_3) p-type and (90% Bi_2Te_3-5% Sb_2Te_3-5%Sb_2Se_3) n-type alloys prepared by hot or cold or sintering pressing method to reveal any precipitates. Both of these alloys, whether grown by the Bridgman method or the travelling heater method, produce bi- or tri- crystals. X-ray orientation of these crystals showed the (111) plane to be lying within 10°-15° of the freezing direction (direction of the crystal ingot axis). Bi_2Te_3 – related pseudo-binary and ternary alloys have been extensively studied in single crystal form[7,8,9,10]. Mzerd et al.[5] have shown that the relative intensities of various peaks obtained by x-ray diffraction of the annealed samples of Sb_2Te_3 are greater than those in the case of unannealed samples and this is due to change in stoichiometry. Francombe[11] has reported that upon heating, the c-axis of the hexagonal unit cell expands more rapidly than the a-axis. Shvangiradze et al.[12] studied the alloys ($Bi_{0.12}Sb_{0.88}$)$_{1-y}Te_y$ (y = 0.57 – 0.615) by the methods of x-ray phase and metallographic analysis. According to the data obtained, alloys with a tellurium content exceeding 60.2 atomic % are two-phase materials; they consist of a matrix phase (the solid solution $Bi_{0.24}Sb_{1.76}Te_3$) and tellurium, whose quantity increases together with the tellurium content in the starting charge. In the two phase region with excess of tellurium, the a and c lattice parameters do not change. However, in alloys with 57-59.4 atomic % Te, the cell parameters decrease. Ha et al.[13] studied the effect of excess tellurium in Bi_2Te_3-Sb_2Te_3 solid solutions grown using the zone melting and Bridgman methods under different growth conditions with the help of x-ray diffraction measurements. Peaks due to elemental Te appeared for the entire length of the ingot when the growth speed was 0.5 mm/min and their intensities increase continuously along the growth direction. However,

these peaks appeared only for the top part of the ingot when the growth speed was 0.1 mm/min regardless of the growth method.

In the present study, Philips PW3710 X-ray diffractometer with copper target has been used for obtaining the powder diffraction pattern of $Bi_xSb_{2-x}Te_3$ (x = 0, 0.2, 0.5, 1) and $In_{0.2}Sb_{1.8}Te_3$ crystals. The x-ray generator was operated at 35 kV and 20 mA. The diffractometer used has a radiation counter to measure the angular position and intensity of the diffracted beam. A recorder automatically plots the intensity of the diffracted beam as the counter moves on a goniometer circle which is in synchronization with the specimen over the selected range of 2θ values as shown in Fig. 2.

Samples from different parts of the crystal were used for obtaining X-ray powder diffractograms. The pattern was obtained for 2θ angles between 20° and 60° in a step size of 0.04°. The time per step was 1 second. The x-rays obtained using the copper target have characteristic radiation $K_{\alpha 1}$ and $K_{\alpha 2}$ lines (K_β filtered out using Ni filter) which occur at wavelengths of about 0.154056 nm and 0.154439 nm, respectively. The PC-APD diffraction software was used to obtain the XRD pattern with $K_{\alpha 2}$ lines eliminated. Hence raw x-ray patterns, as well as the patterns after removal of $K_{\alpha 2}$ wavelength, were obtained. An XRD program (POWD Version 2.2) was used for indexing the pattern on the basis of the hexagonal unit cell and lattice parameters, as reported by Smith et al.[14], for the solid solution of Bi_2Te_3 - Sb_2Te_3.

Fig. 3 shows an X - ray diffractogram of the crystal powder of $Bi_xSb_{2-x}Te_3$ (x = 0, 0.2, 0.5, 1). The pattern consists of well-defined sharp diffraction lines indicating good crystallinity of the specimen. Table 3 shows the indexing of the diffraction pattern. The peaks in the pattern of Sb_2Te_3 were compared with those in the JCPDS data card and were found to match readily. Table 4 shows the values of the a and c lattice parameters evaluated from the X ray data. The values of the lattice parameters obtained for Sb_2Te_3 crystal: a = 0.426 nm and c = 3.0427

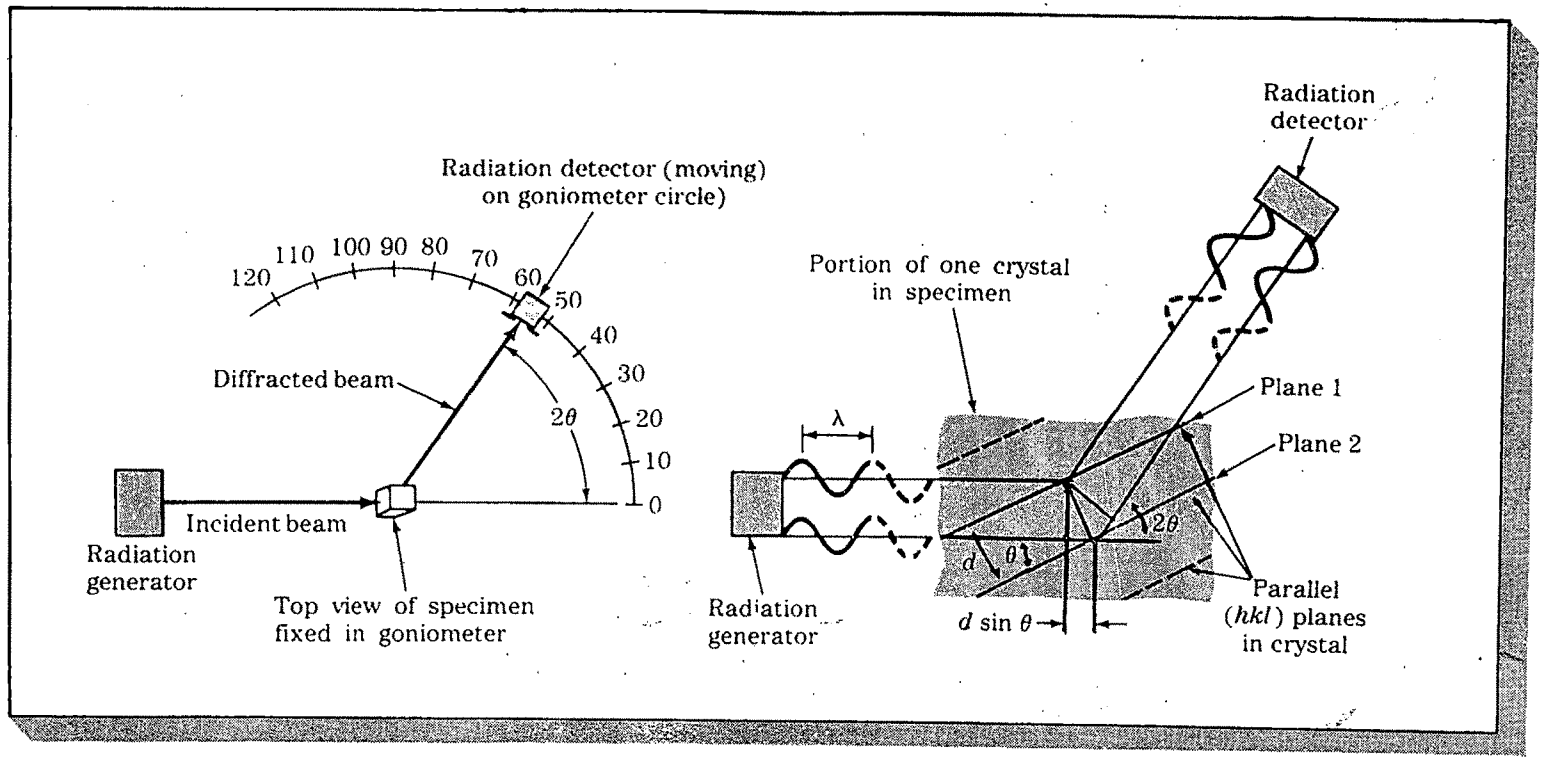

Fig. 2. Schematic illustration of the diffractometer method

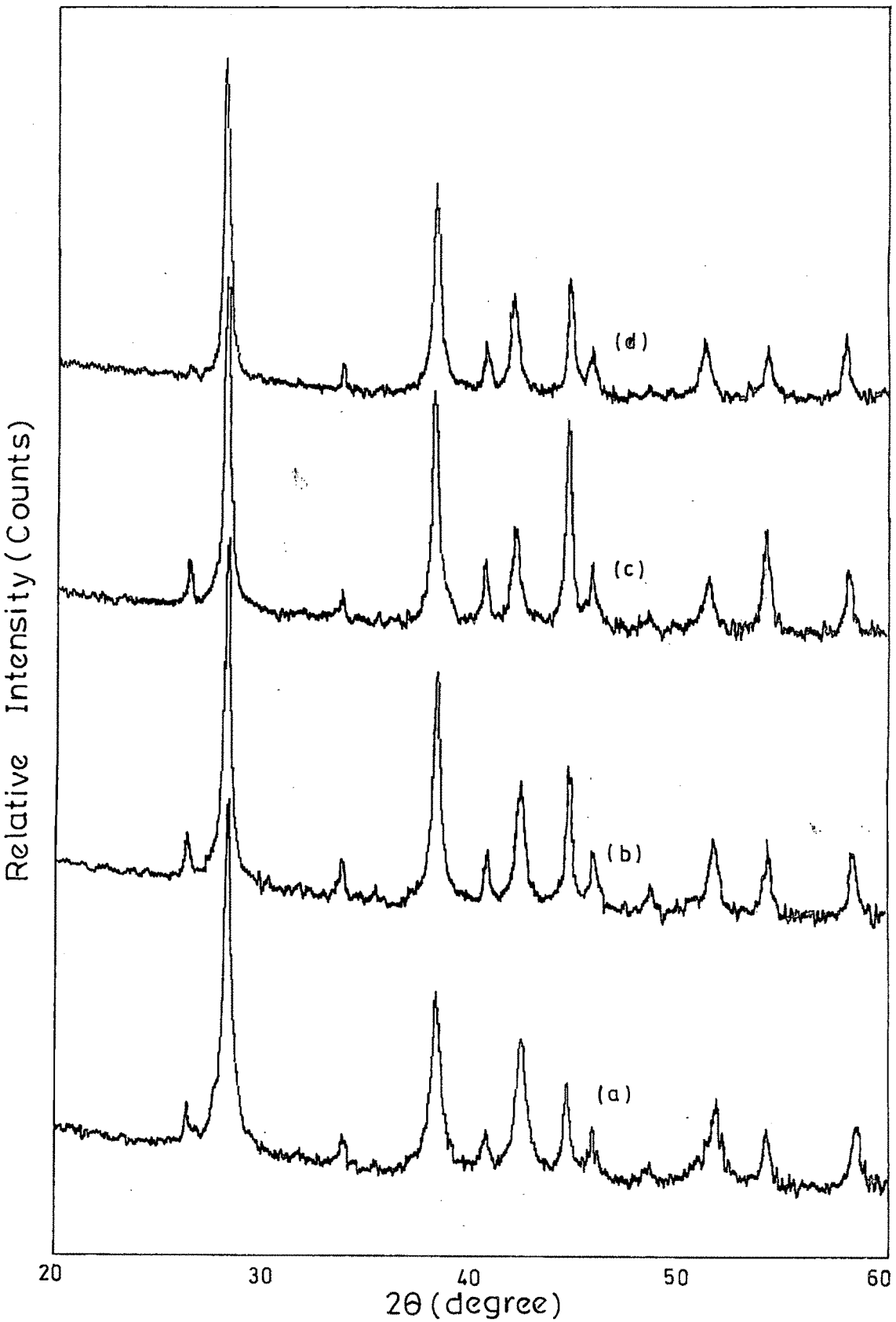

Fig. 3 X-ray Powder Pattern of (a) Sb_2Te_3 (b) $Bi_{0.2}Sb_{1.8}Te_3$ (c) $Bi_{0.5}Sb_{1.5}Te_3$ (d) $BiSbTe_3$

Table 3

Indexing of $Bi_xSb_{2-x}Te_3$ (x= 0,0.2,0.5,1)

Sb_2Te_3		$Bi_{0.2}Sb_{1.8}Te_3$		$Bi_{0.5}Sb_{1.5}Te_3$		$BiSbTe_3$	
d Å	(h k l)	d Å	(h k l)	d Å	(h k l)	d Å	(h k l)
3.383	(0 0 9)	3.383	(0 0 9)	3.381	(0 0 9)	3.379	(0 0 9)
3.157	(1 0 5)	3.157	(1 0 5)	3.166	(1 0 5)	3.182	(1 0 5)
2.651	(1 0 8)	2.651	(1 0 8)	2.656	(1 0 8)	2.664	(1 0 8)
2.349	(1 0 10)	2.349	(1 0 10)	2.356	(1 0 10)	2.358	(1 0 10)
2.215	(10 11)	2.215	(10 11)	2.219	(1 0 11)	2.222	(1 0 11)
2.130	(1 1 1)	2.130	(1 1 1)	2.146	(1 1 0)	2.155	(1 1 0)
2.030	(0 0 15)	2.030	(0 0 15)	2.029	(0 0 15)	2.027	(0 0 15)
1.964	(1 0 13)	1.964	(1 0 13)	1.982	(1 0 13)	1.982	(1 0 13)
1.766	(2 0 5)	1.766	(2 0 5)	1.778	(2 0 5)	1.784	(2 0 5)
1.692	(1 0 16)	1.692	(1 0 16)	1.693	(1 0 16)	1.675	(2 0 8)
1.578	(1 1 13)	1.578	(1 1 13)	1.587	(0 2 10)	1.591	(2 0 10)

Table 4

Lattice Parameters of $Bi_xSb_{2-x}Te_3$ (x= 0,0.2,0.5,1)

Crystal	a nm	c nm
Sb_2Te_3	0.426	3.0427
$Bi_{0.2}Sb_{1.8}Te_3$	0.426	3.0426
$Bi_{0.5}Sb_{1.5}Te_3$	0.429	3.0423
$BiSbTe_3$	0.4323	3.0427

nm are in good agreement with the values obtained by Horak et al.[4]. While the a lattice parameter has been observed to increase with the increase in the concentration of Bi in Sb_2Te_3, the c lattice parameter remains constant and the results are in fair agreement with those reported by Smith et al.[14] for the complete range of the solid solution (Fig. 4).

Typical X-ray diffraction spectra of Sb_2Te_3, $Bi_{0.2}Sb_{1.8}Te_3$ and $In_{0.2}Sb_{1.8}Te_3$ crystal powders are shown in Fig. 5. The patterns show no new peaks introduced by Bi and In indicating that Bi and In have assumed substitutional positions in the Sb_2Te_3 lattice. No reflections corresponding to the free elements, if any, were detected in the diffraction pattern [Table 5]. The lattice parameters a and c were refined and recalculated by least squares method for $In_{0.2}Sb_{1.8}Te_3$ and $Bi_{0.2}Sb_{1.8}Te_3$. The lattice parameters obtained are given in Table 6. Rosenberg et al.[15] have observed that with increasing In concentration, the c parameter first increases slightly and then decreases for $x > 0.3$; the a parameter, on the other hand, decreases over the whole range. The variation of these parameters with indium content in the Sb_2Te_3-In_2Te_3 alloys is shown in Fig. 6. The x-ray data obtained by them show the maximum solubility of In_2Te_3 in the Sb_2Te_3 structure to be about 45%. The second phase appearing in samples with larger concentrations was identified as In_2Te_3. However, in the present case, no change in the lattice parameter indicates that Bi and In substitute Sb in Sb_2Te_3. This should be expected since the atomic radii of Bi and In are within 5% of the atomic radius of Sb.

SECONDARY ION MASS SPECTROSCOPY STUDY

Secondary Ion Mass Spectrometry (SIMS) is capable of providing information of purity, dopant distribution and stoichiometry in the material. This technique can achieve high detection sensitivities in very small analytical volumes and for a wide range of elements (almost the entire periodic table).

Glazov et al[16] analyzed the distribution of the components using Cameca microanalyzer in cross sections of samples of $Bi_2Te_{2.4}Se_{0.6}$ and $Bi_{0.52}Sb_{1.48}Te_3$

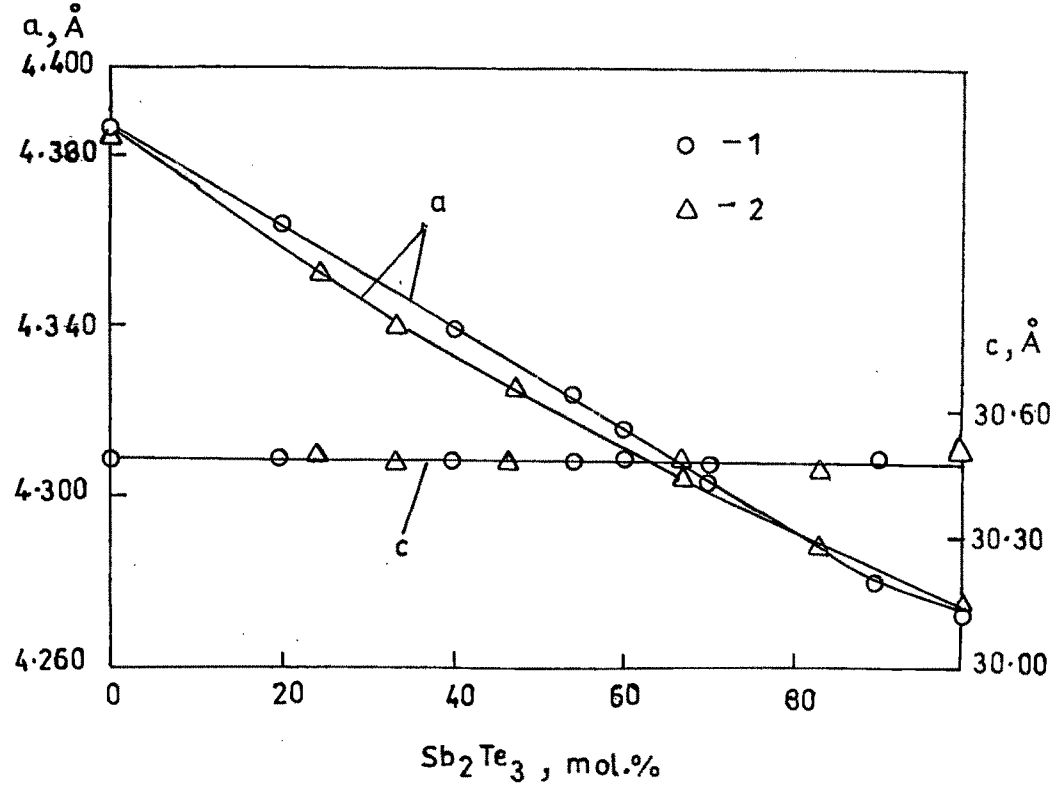

Fig. 4. Lattice parameters of Bi_2Te_3–Sb_2Te_3 solid solutions

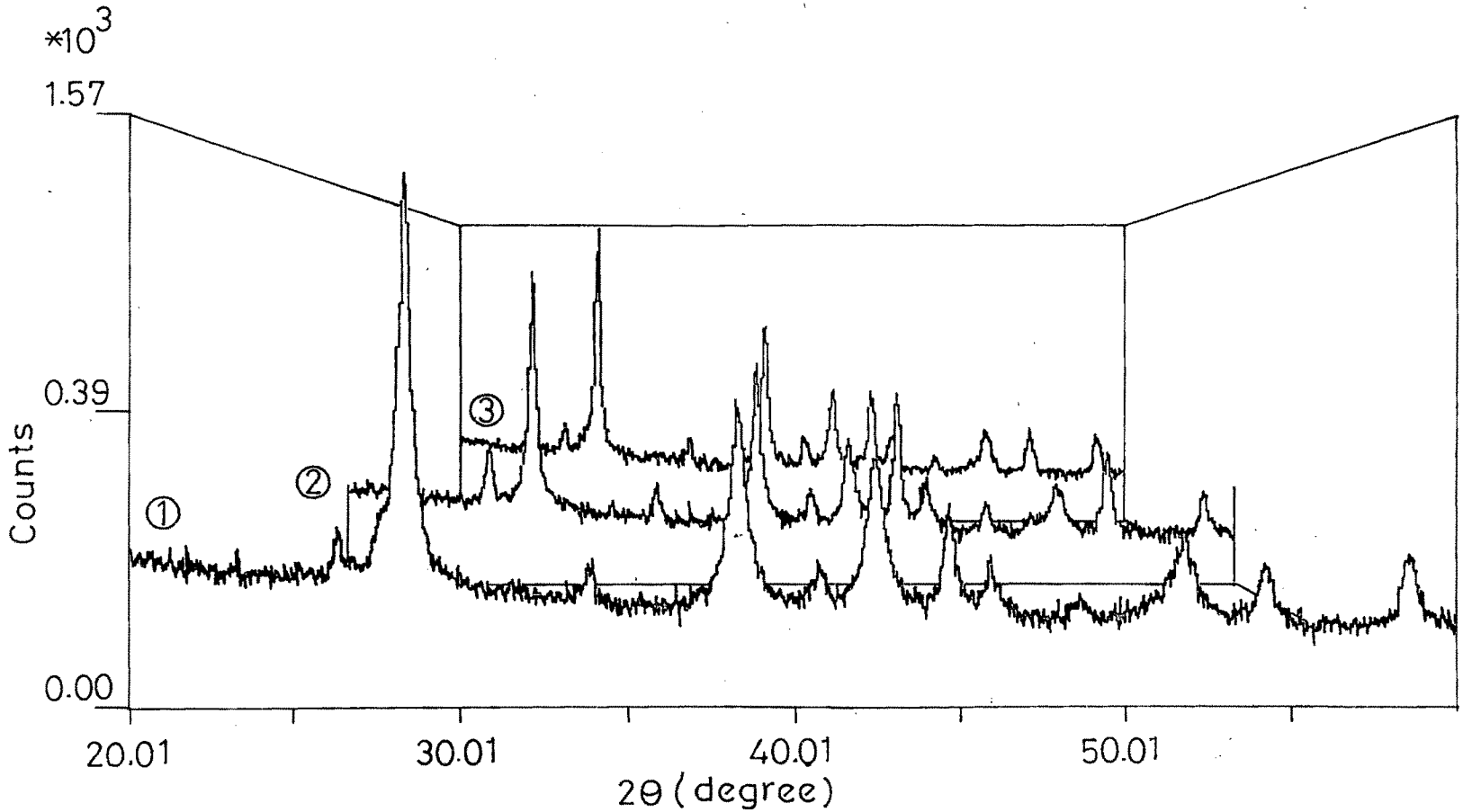

Fig. 5 X-Ray Diffractogram of ① Sb_2Te_3 ② $In_{0.2}Sb_{1.8}Te_3$ ③ $Bi_{0.2}Sb_{1.8}Te_3$

TABLE 5.

Diffraction data of Sb_2Te_3, $Bi_{0.2}Sb_{1.8}Te_3$ and $In_{0.2}Sb_{1.8}Te_3$

Sb_2Te_3 (standard data)		Sb_2Te_3	$Bi_{0.2}Sb_{1.8}Te_3$	$In_{0.2}Sb_{1.8}Te_3$
d Å	(h k l)	d Å	d Å	d Å
3.383	(0 0 9)	3.3739	3.3833	3.3801
3.157	(1 0 5)	3.1531	3.1608	3.1477
2.651	(1 0 8)	2.6532	2.6543	2.6459
2.349	(1 0 10)	2.3499	2.3514	2.3466
2.215	(10 11)	2.2163	2.2171	2.2127
2.130	(1 1 1)	2.1291	2.1353	2.1269
2.030	(0 0 15)	2.0293	2.0308	2.0293
1.964	(1 0 13)	1.9752	1.9818	1.9767
1.766	(2 0 5)	1.7674	1.7708	1.7652
1.692	(1 0 16)	1.6913	1.6922	1.6923
1.578	(1 1 13)	1.5752	1.5824	1.5758

Table 6.

Lattice Parameters of Sb_2Te_3, $Bi_{0.2}Sb_{1.8}Te_3$ and $In_{0.2}Sb_{1.8}Te_3$

Crystal	a nm	c nm
Sb_2Te_3	0.426	3.0427
$Bi_{0.2}Sb_{1.8}Te_3$	0.426	3.0426
$In_{0.2}Sb_{1.8}Te_3$	0.426	3.0428

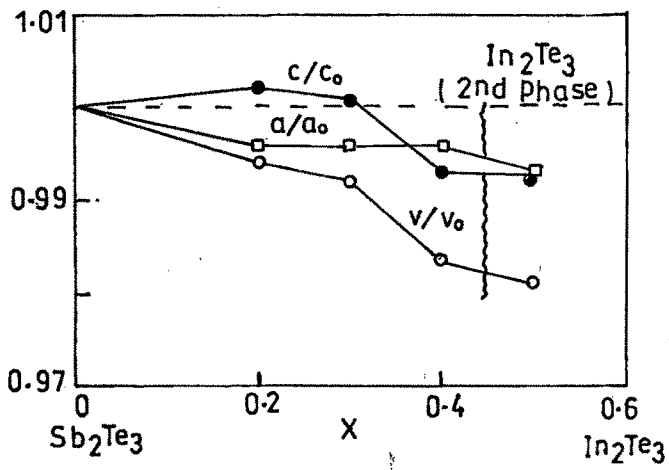

Fig. 6. Lattice parameters of Sb_2Te_3-In_2Te_3 solid solutions

prepared by ultrafast cooling. They found high variation in chemical homogeneity on the cross sections.

The SIMS instrument used in the present study is a CAMECA IMS-4f double-focussing magnetic sector ion microanalyzer. The basic components of a SIMS instrument are illustrated in Fig. 7. The main elements of a SIMS apparatus are: primary ion source, primary optics comprising ion extraction and acceleration, sample stage, secondary optics consisting of secondary ion acceleration, energy selector and mass spectrometer; detector and associated electronics. A magnetic sector analyzer separates the beam of secondary ions into its component parts according to their mass/charge ratios.

Due to the penetration of the energetic primary ions into the sample surface and associated damage by ion-beam mixing, knock-on effect, collision cascades, etc., there is a finite depth resolution associated with the SIMS technique. In effect, a relatively uniform amorphous layer of mixed composition (including substantial amounts of the implanted primary ion species) is formed on the sample surface (after an initial equilibration period). The secondary ions (and neutral atoms) are sputtered out of the top atomic layers of this mixed region. The thickness of the layer is determined largely by the range of the implanted primary ions and hence depends on their energy and incident angle. Thus the crystal can be characterized in terms of elemental concentration versus depth.

The measurements were made using Caesium primary ion bombardment, with a net impact energy ~ 10 keV. Nominal beam currents were in the range 101.95 - 106.03 nA. The primary ion beam was rastered over an area of about 250 μm^2 of the cleavage surface and the detected secondary ions were extracted from the central area of the crater. The depth profiles were obtained in the form of ion counts per unit time.

Fig. 8 shows a SIMS profile of $BiSbTe_3$ crystal. The uniformity of element distribution up to a depth of 10 μm, which is normally the limit of the SIMS technique, is sufficiently indicative of the homogeneity of the sample since the

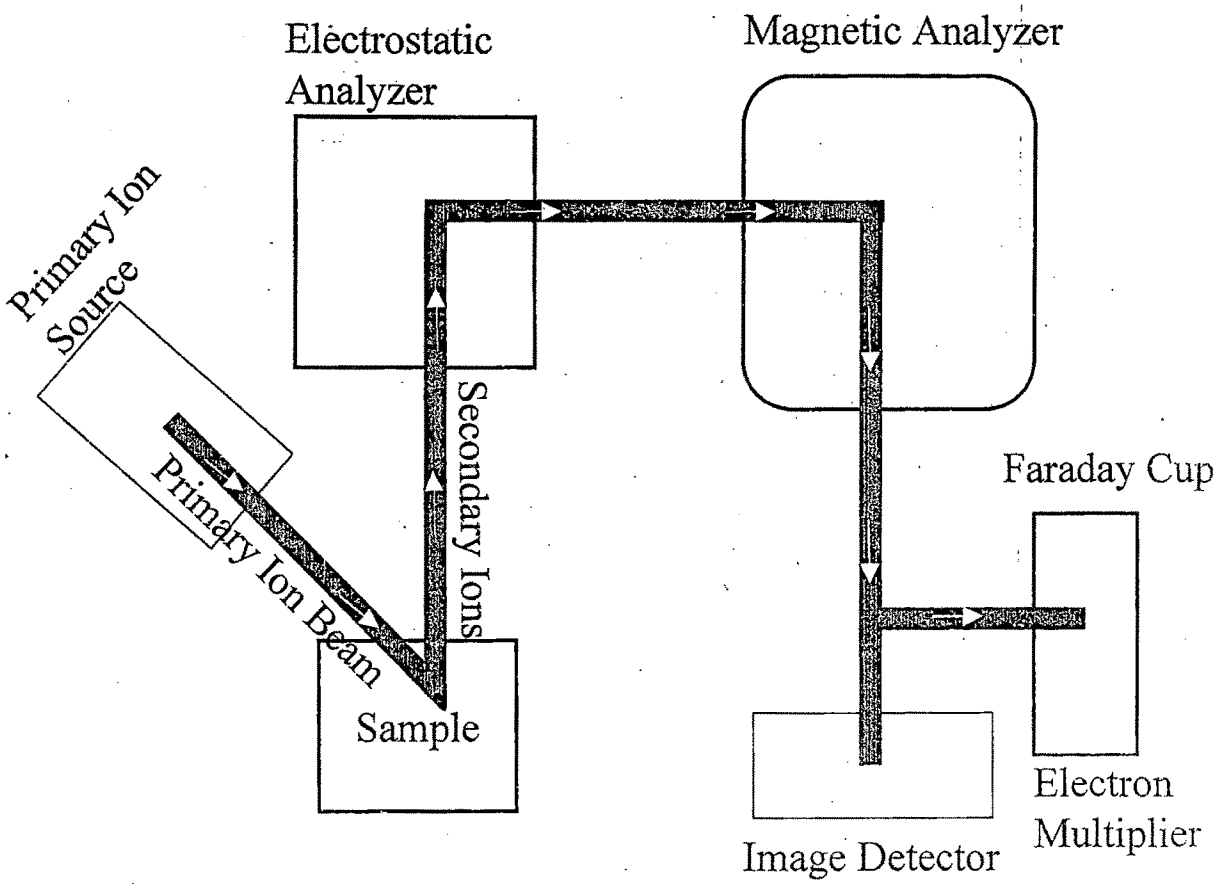

Fig. 7. Schematic of a magnetic sector SIMS instrument

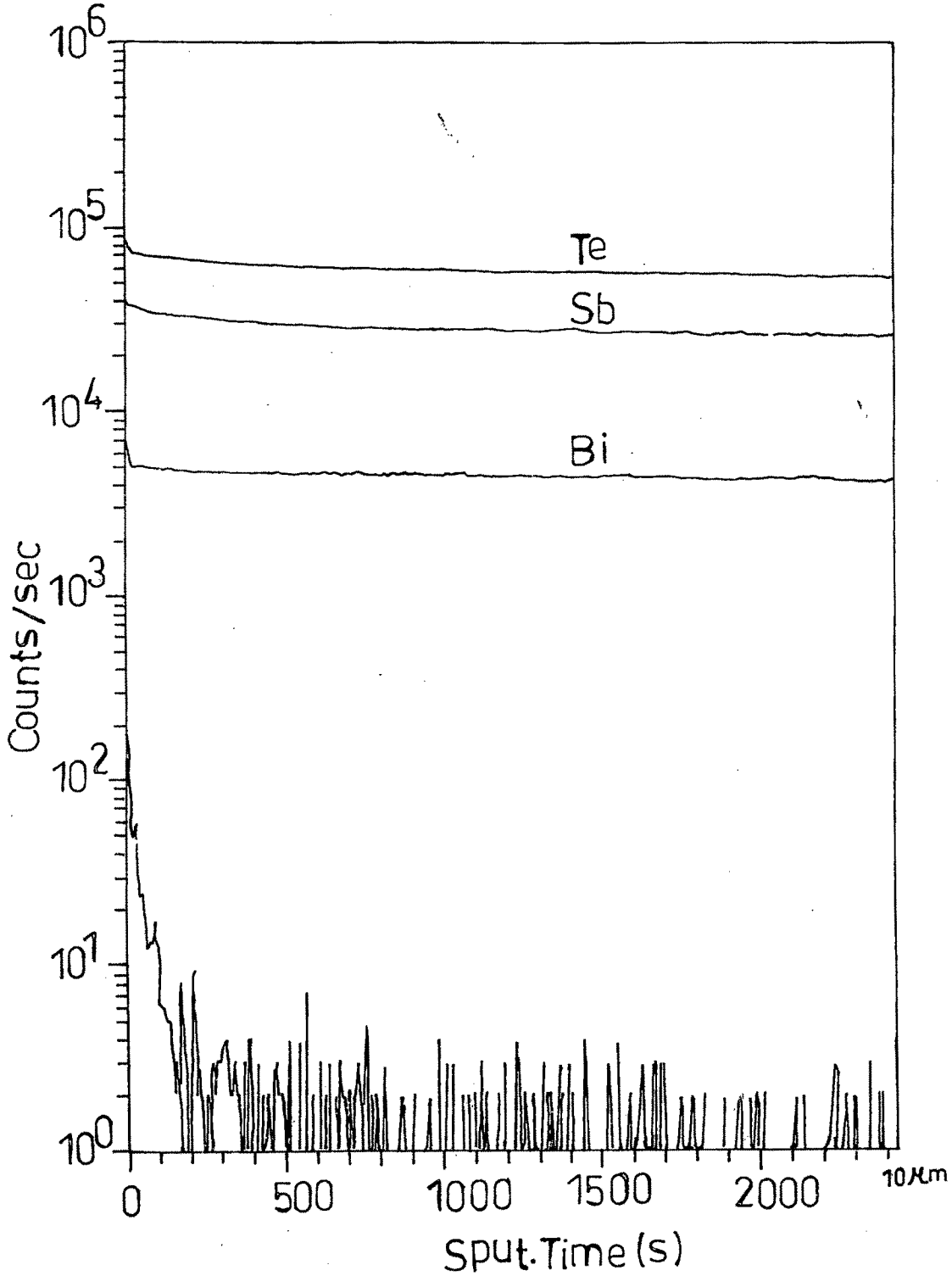

Fig. 8. SIMS depth profile of $BiSbTe_3$ crystal

conditions prevalent at the surface would be more prone to inducing inhomogeneity than those in the interior of bulk. Undesired impurities present at the interface of the sample are also indicated by the low lying profile structure. This is pronounced only up to a depth of about 0.3 μm and must have been caused by associated ion-beam mixing damage, etc. discussed above.

CONCLUSION

1) EDAX analysis indicates near stoichiometry of the crystals prepared. However, the presence of silicon is unavoidable due to the silica crucible.
2) The X-ray diffractometry study indicates the substitutional effect of In and Bi at the antimony sites in Sb_2Te_3 and also the substitutional effect of Bi at the Sb sites for the range of solid solution of Bi_2Te_3-Sb_2Te_3 under study.
3) The homogeneity of the samples as analysed by the SIMS technique is quite satisfactory.

REFERENCE

[1] Ivanova, L. D., Konstantinova, M. S., Granatkina, Yu. V. and Sidorov, Yu. A. (1991) Neorg. Mater. 27, 699.

[2] Mavlonov, Sh. and Sherov, P. N. (1986) Neorg. Mater. 22, 52.

[3] Ivanova, L. D., Granatkina, Yu. V., Polikarpova, N. V. and Smirnova, E. I. (1992) Neorg. Mater. 28, 759.

[4] Horak, J., Drasar, C., Novotny, R., Karamazov, S. and Lostak, P. (1995) Phys. Stat. Sol. (a) 149, 549.

[5] Mzerd, A., Sayah, D., Tedenac, J. C. and Boyer, A. (1994) Phys. Stat. Sol. (a) 141, 183.

[6] Amin, P. A. A., Al-Ghaffari, A. S. S., Issa, M. A. A. and Hassib, A. M. (1992) J. Mat. Sci. 1250.

[7] Rosi, F. D., Abeles, B. and Jensen, R. V. (1959) J. Phys. Chem. Solids 10, 191.

[8] Yim, W. M. and Rosi, F. D. (1972) Solid State Electronics 15,1121.

[9] Birkholz, U. (1958) Z. Naturforsch. 13a, 78.

[10] Goldsmid, H. J. (1961) J. Appl. Phys. 32, 2198.

[11] Francombe, M. H. (1958) Brit. J. Appl. Phys. 9, 415.

[12] Shvangiradze, R. R., Bigvava, A. D., Korobov, V. K., Kunchuliya, E. D., Kutsiya, A. A. and Tsintsadze, N. A. (1988) Neorg. Mater. 24, 1799.

[13] Ha, H. P., Cho, Y. W. Byun, H. Y. and Shim, J. D. (1994) J. Phys. Chem. Solids 55, 1233.

[14] Smith, M. J., Knight, R. J. and Spencer, C. W. (1962) J. Appl. Phys. 33, 2186.

[15] Rosenberg, A. J. and Strauss, A. J. (1961) J. Phys. Chem. Solids 19, 105.

[16] Glazov, V. M. and Yatmanov, Yu. V. (1986) Neorg. Mater. 22, 36.